Weldability of Fe-36% Ni Alloy (Report II)

— Effect of Chemical Composition on Reheated Hot Cracking in Weld Metal —

Fukuhisa MATSUDA*, Hiroji NAKAGAWA**, Setsuji MINEHISA***,
Nobuharu SAKABATA***, Akio EJIMA**** and Kiyohiko NOHARA****

Abstract

Studies are made on chemical compositions of Fe-36% Ni alloy for membrane-type LNG tanks to prevent ductility-dip crack in weld metal. Cross-bead type hot cracking test are conducted for 24 different composition alloy samples. The relationship between chemical composition and total crack length is studied by regression analysis. Materials having good properties against the ductility-dip crack are produced on practical production line and are used for practical fabrication of model tanks. Conclusions thus obtained are as follows: 1) S, O, N and Al are the elements promoting ductility-dip crack, while P shows a slight trend of promoting the crack. Si and Mn function as the elements inhibiting the crack formation. 2) By using the basic elements and impurity elements contained in the alloys, an estimating equation for the total crack length in Cross-bead cracking test is obtained. 3) Materials having good properties against the crack are produced on practical production line and are used for practical fabrication of model tanks. Obtained results are favorable.

KEY WORDS: (Hot Cracking) (Controlled Expansion Alloys) (Containers)

1. Introduction

In Fe-36% Ni alloy (hereafter referred to as "Invar") used for LNG tanks etc. as a low temperature material, hot crack occurs in some cases during welding, since the alloy has full austenite structure; particularly ductility-dip crack easily occurs in reheated weld metal in such joints as with multipass beads or repair welds. In the previous paper[1)], Cross-bead type hot cracking tests were conducted and the cracking phenomena were studied. As the results, the following have been revealed: a) The ductility-dip crack occurs in the reheated weld metal with a peak temperature of 800 to 1300°C. b) The crack location is migrated grain boundary after solidification, and its fractographic feature shows intergranular mode. c) All the feature of the crack shows a behavior of ductility-dip crack, not a behavior of liquation crack. However, little knowledge was obtained as to which element causes the crack and which mechanism acts.

Therefore, as the second part of the studies, influence of the elements contained in the alloy on the crack has been studied, first of all, by means of regression analysis, particularly to identify bad elements. Then an estimating equation has been prepared on the total crack length in Cross-bead test. Furthermore, the materials judged to have favorable properties against the ductility-dip crack through this study have been practically applied to fabricate model tanks of membrane type, and their properties against the ductility-dip crack have been confirmed.

2. Experimental Procedures

2.1 Materials used

Table 1 shows the chemical compositions of materials used, where two materials (No. 23 and 24) are commercial ones and other 22 kinds of materials are tentative ones having different chemical compositions from one another. The tentative materials were prepared by vacuum melting into 50kg ingots, and formed into thin sheets of 1.5mm thickness by cold rolling for the test use. In the tentative materials, basic components of C, Si and Mn together with minor elements of P, S, O, N and Al were varied.

* Professor
** Research Instructor
*** Hitachi Zosen Corp.
**** Kawasaki Steel Corp.

Transactions of JWRI is published by Welding Research Institute of Osaka University, Ibaraki, Osaka 567, Japan

Table 1 Chemical compositions of materials used

Item No.	Chemical composition (wt.%)								
	C	Si	Mn	P	S	N	O	Al*	Ni
1	0.031	0.20	0.50	0.002	0.0011	0.0008	0.0034	0.009	36.25
2	0.029	0.21	0.38	0.004	0.0006	0.0008	0.0026	0.013	36.30
3	0.029	0.19	0.37	0.005	0.0025	0.0013	0.0040	0.003	36.28
4	0.025	0.17	0.35	0.004	0.0004	0.0007	0.0018	0.008	35.81
5	0.031	0.17	0.35	0.009	0.0005	0.0008	0.0018	0.008	35.93
6	0.031	0.18	0.35	0.004	0.0005	0.0010	0.0019	0.008	36.05
7	0.034	0.18	0.35	0.002	0.0005	0.0010	0.0016	0.002	35.93
8	0.031	0.18	0.46	0.001	0.0005	0.0045	0.0014	0.006	35.81
9	0.017	0.19	0.36	0.001	0.005	0.0017	0.0036	0.001	36.20
10	0.032	0.20	0.36	0.001	0.008	0.0011	0.0018	0.001	36.24
11	0.033	0.19	0.36	0.003	0.005	0.0011	0.0012	0.001	36.28
12	0.033	0.19	0.35	0.003	0.005	0.0035	0.0021	0.001	36.05
13	0.028	0.19	0.35	0.004	0.004	0.0047	0.0038	0.001	34.97
14	0.035	0.51	1.04	0.0005	0.001	0.0008	0.0014	0.004	35.8
15	0.027	0.49	1.03	0.0048	0.0010	0.0007	0.0022	0.001	35.6
16	0.027	0.50	1.02	0.0005	0.0055	0.0007	0.0013	0.001	35.7
17	0.04	0.49	1.00	0.0008	0.0011	0.0049	0.0019	0.001	35.8
18	0.049	0.49	1.01	0.012	0.0010	0.0086	0.0069	0.001	35.8
19	0.036	0.46	1.03	0.0005	0.0010	0.0019	0.0050	0.001	35.7
20	0.027	0.20	0.31	0.002	0.0031	0.0017	0.0026	0.001	36.0
21	0.029	0.21	0.33	0.001	0.0013	0.0013	0.0027	0.001	36.1
22	0.030	0.16	0.33	0.005	0.0014	0.0020	0.0025	0.003	35.8
23	0.030	0.24	0.34	0.002	0.002	0.0044	0.0043	0.023	35.04
24	0.034	0.26	0.36	0.012	0.0018	0.005	0.0022	0.026	35.80

*: soluble

2.2 Hot cracking test

Cross-bead type hot cracking test was used as in the previous paper[1]. The testing method is explained below: Prior to the cracking test, first pass welding was done as shown in **Fig. 1**, where the width of weld bead in the back surface was nearly the same as that in the surface. In this case the amounts of oxygen and nitrogen may vary depending on the welding conditions and shielding conditions due to gas absorption. Therefore the welding was done in a chamber filled with pure argon. **Figure 2** shows the general appearance of the chamber. After evacuating the chamber up to 10^{-3} torr., 99.99% pure argon was filled into the chamber. As the result remaining oxygen content was less than 20ppm. **Table 2(a)** shows the welding conditions of the first pass with TIG-arc process. Oxygen and nitrogen contents in the weld metal were analyzed and utilized for the multiple linear regression analysis mentioned later.

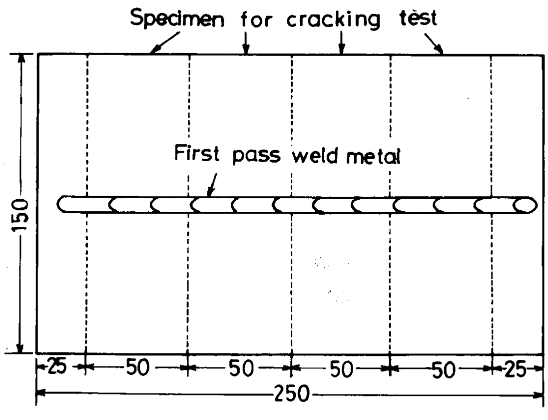

Fig. 1 Specimen configuration for first pass welding

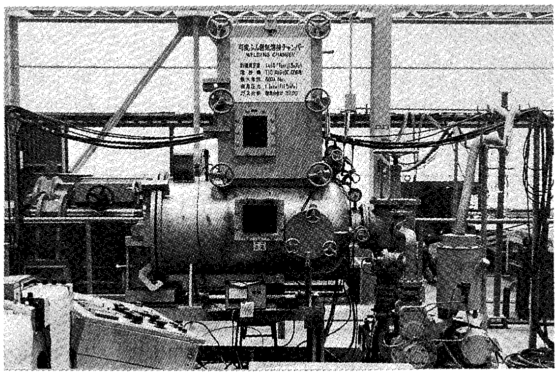

Fig. 2 General view of welding chamber used

Table 2 TIG welding conditions

Pass No.	Arc voltage (V)	Welding current (A)	Welding speed (mm/min)
(a) First pass	7	40	100
(b) Second pass	11	60	100

After welding the first pass, the specimen for the

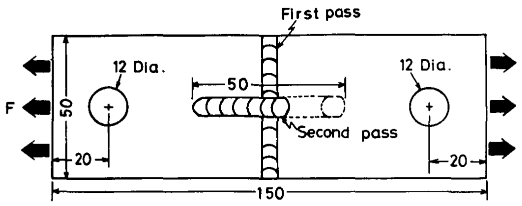

Fig. 3 Specimen configuration for Cross-bead test and illustration of its principle

cracking test was cut off along the broken line in Fig. 1. The detailed configuration of the testing specimen is shown in **Fig. 3**. The second pass welding was done with TIG-arc process perpendicularly to the first pass, with argon back shielding. Table 2(b) shows the welding conditions. During the welding, constant load (F) was applied to the welding direction of the second pass. The load was adjusted so that the average stress was 5, 10 and 15kgf/mm^2, respectively. After the completion of the welding, the total length of the all cracks in the first pass, namely the total crack length, was measured with an optical microscope in magnification of 100.

2.3 Analysis on effects of chemical composition on crack

Correlation between the chemical composition and the total crack length was studied by regression analysis. Also an estimating equation for the total crack length was studied by multiple linear regression. In these regressions, oxygen and nitrogen contents in both base metal and weld metal by the first pass were used and compared.

2.4 Application to fabrication

The alloys which was judged to be favorable in the property against the crack was produced on the practical production line and used for the fabrication of model tanks of membrane type. The model tank has a capacity of about 300m^3 and is of a double-structure with primary and secondary barriers.

3. Experimental Results and Discussions

3.1 Results in cracking test

Figure 4 shows the typical example of the macrostructure around the cracks (mark C), which occurred in the weld metal of first pass reheated by the second pass. In the previous paper[1] the authours showed that the crack occurs in the reheated weld metal with a peak temperature of 800 to 1300°C. According to the results in this report with many specimens, however, it was observed that the crack occurs in the reheated weld metal

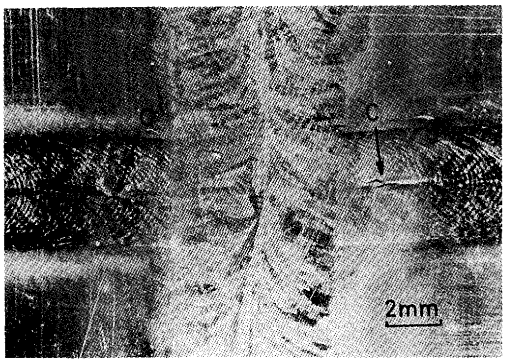

Fig. 4 Macrostructure around cracks after Cross-bead test

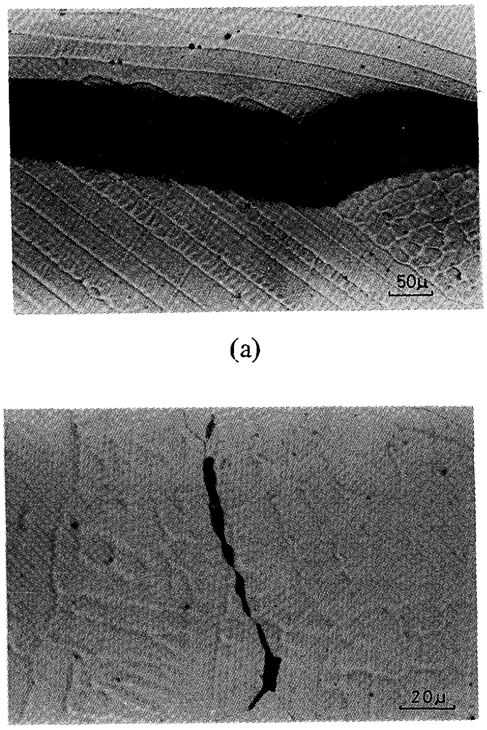

(a)

(b)

Fig. 5 Examples of microstructure around crack

with a peak temperature of 600 to 1300°C in crack-susceptible specimens, and with a peak temperature of 900 to 1000°C in crack-insusceptible specimens. **Figure 5** shows microstructures around the crack, which occurred along migrated grain boundary after solidification. The opening of crack in Fig. 5(b) is obscure, but clear in SEM observation. Therefore, the total crack length measured included such a crack as seen in Fig. 5(b).

Table 3 summarizes the total crack length (L). The total crack length increased together with the increase in the applied stress. Generally the total crack length increases suddenly when the applied stress exceeds 10kgf/

Table 3 Results of Cross-bead hot cracking test

Item No.	Total crack length, L (mm)			
	0 (kg/mm²)	5 (kg/mm²)	10 (kg/mm²)	15 (kg/mm²)
1	-	-	0	0.68
2	-	-	0	1.4
3	-	-	0.06	5.81
4	-	-	0.11	2.94
5	-	-	0	0.92
6	-	-	0	0.96
7	-	-	0	0.18
8	-	-	0	3.01
9	-	0.43	2.17	48.5
10	0	0.63	1.42	37.59
11	-	0	0.29	33.63
12	-	0	0.21	35.36
13	-	0	0.14	37.57
14	0	0	0	11.08
15	-	0	0	1.58
16	0	0	0	2.93
17	-	0	0	2.30
18	-	0	1.2	25.47
19	-	0	0.1	0.97
20	-	0	1.6	49.33
21	-	0	0	7.24
22	-	0	0	8.62
23	2.11	2.84	5.14	73.89
24	-	9.29	14.78	63.09

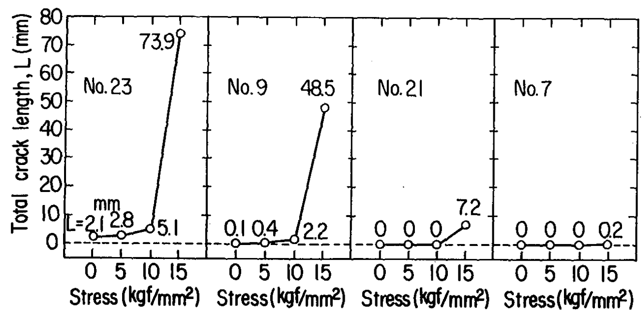

Fig. 6 Relation between applied stress and total crack length in susceptible and insusceptible specimens to crack.

mm². **Figure 6** shows the typical examples. Comparing the results in Fig. 6 with the chemical compositions in Table 1, the following trends are seen: The oxygen, nitrogen and aluminum contents in the specimen No. 23 are relatively high. The sulphur and oxygen contents in the specimen No. 9 are relatively high. However, these elements are relatively low in the specimens No. 7 and 21, which showed small total crack length.

3.2 Effect of chemical composition on crack

Table 3 and Fig. 6 suggest that chemical composition has much effect on the ductility-dip crack. Therefore the effects of chemical compositions was studied by means of regression analysis. Concerning the oxygen and nitrogen contents, it would be better to use the contents in the weld metal of the first pass in principle, but it would be better to use the contents in the base metals for the steel

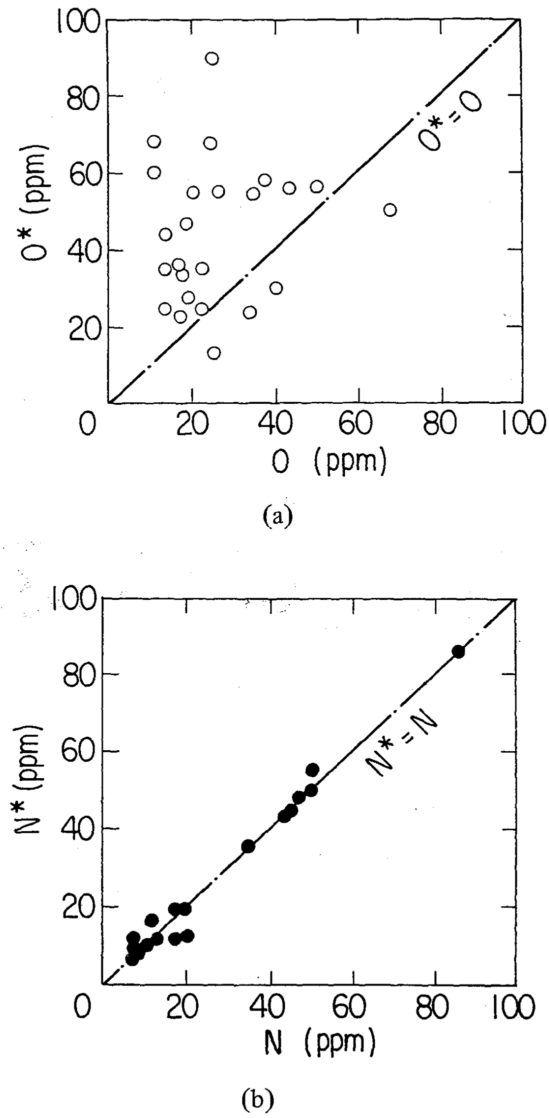

Fig. 7 Comparison between gas contents in base metal (oxygen: O, nitrogen: N) and those in weld metal (oxygen: O*, nitrogen: N*)

maker. Therefore the contents in both the weld metal and the base metal were analyzed.

Figure 7 shows the relation between the oxygen and nitrogen contents in the base metals (hereafter referred to as O and N, respectively) and these contents in the weld metal of first pass (O* and N*, respectively). There is no correlation between O and O*, and O* is generally higher than O. This means that oxygen is generally absorbed during welding. On the other hand, N* well agrees with N.

Table 4 shows the correlation coefficient (r) of all elements in relation to the total crack length (L) under the condition of 15 kgf/mm² obtained by linear regression analysis. Table 4 means that S, O(O*), N(N*) Al and P are the promoting elements of the crack, while Si and Mn are the inhibiting elements of the crack. **Table 5**

Table 4 Correlation coefficient (r) of element (x) in relation to total crack length (L) by linear regression analysis

No.	Element	Correlation coefficient (r) (%)	
		Base metal	Weld metal
1	C	−11.2	—
2	Si	−19.5	
3	Mn	−34.1	
4	P	17.0	
5	S	46.9	
6	O (O*)	23.2	35.8
7	N (N*)	42.0	43.2
8	Ni	−10.9	—
9	Al	40.0	

$$r = \frac{\sum_{i=1}^{n} (x_i - \bar{x})(L_i - \bar{L})}{(n-1) S_x \cdot S_y}$$

$\bar{x}, \bar{L}$: means
S_x, S_y : standard deviations

Table 5 Summarized tendencies of elements in relation to crack

⊕	S, O (O*), N (N*), Al, P
⊖	Mn, Si
×	C, Ni

⊕ : to promote hot cracks
⊖ : to inhibit hot cracks
× : little effect on hot cracks

shows the summary of the effects of elements. Generally speaking, these elements don't act to the crack individually, but act in mutual correlation. For instance, Mn easily couples with S and O, and Si easily couples with O. **Table 6** shows the correlation coefficient (r) of simple combinations of these elements obtained by linear regression analysis, where the combination P + 3S was quoted from

Table 6 Correlation coefficient of expected simple combination of elements in relation to total crack length by linear regression analysis

No.	Function	Correlation coefficient (r) (%)	
		Base metal	Weld metal
1	P + 3S	42.7	—
2	S / Mn	58.2	
3	O (O*)/Mn	52.5	52.6
4	{S+O(O*)}/ Mn	68.9	65.3
5	O (O*)/(Si+Mn)	45.6	48.4
6	P+N(N*)+{S+O(O*)}/ Mn	62.0	76.9

O*, N* : Weld bead

Ref. 2). However, any combination has not so high correlation coefficient in linear regression.

Thus, multiple linear regression was conducted by taking account of coefficient of each element or combination. **Table 7** shows the results. The first equation in

Table 7 Multiple correlation coefficient of proper functions in relation to total crack length by multiple linear regression analysis

No.	Function	Multiple correlation coefficient (R^2) (%)	
		Base metal	Weld metal
1	P+N(N*)+{S+O(O*)}/ Mn+Al	77.2	84.3
2	C+Si+Mn+P+S+O(O*)+N(N*)+Ni+Al	83.8	86.2

O*, N* : Weld bead Stress = 15 kgf/mm²

Table 7 was prepared by adding Al to the sixth equation in Table 6 and furthermore by adding coefficient to each term. The second equation in Table 7 was prepared by multiple regression analysis of all elements. Among the results in Tables 6 and 7, the second equation in Table 7 gives the highest correlation. Comparing the effects of O(N) with O*(N*), O*(N*) as a matter of course gives a higher correlation. (R^2 = 86.2) **Table 8** shows the results

Table 8 Estimating equation for total crack length under the condition of applied stress of 15kgf/mm², obtained by multiple linear regression analysis (content: wt. % x 100).

$$L_{cal} = \alpha_1 C + \alpha_2 Si + \alpha_3 Mn + \alpha_4 P + \alpha_5 S + \alpha_6 O(O^*) + \alpha_7 N(N^*) + \alpha_8 Ni + \alpha_9 Al + \beta$$

Metal	α_1	α_2	α_3	α_4	α_5	α_6	α_7	α_8	α_9	β
Base Metal	−6.31	2.79	−1.41	−1.13	44.48	40.98	17.71	0.001	5.13	7.84
Weld Metal	−6.50	2.06	−1.07	−0.87	30.11	45.26	39.95	0.04	12.41	-151.42

(Stress : 15 kgf/mm²)

of multiple regression analysis of all the elements under the condition of applied stress of 15kgf/mm², where the coefficient of P is a negative value perhaps due to its weak accelerating effect on the crack.

Figure 8 compares the calculated total crack length (L_{cal}) by the equation in Table 8 with the measured value (L_{exp}) by Cross-bead test. Good correspondence is seen between the calculated and measured values.

3.3 Application to practical fabrication

It has been shown from the results above mentioned that the ductility-dip crack has the following characteristics: 1) The total crack length depends on the applied stress, and suddenly increases when the stress exceeds 10kgf/mm². 2) The total crack length depends on the chemical composition, and the reduction of S, O(O*), N(N*), Al and P effectively extinguish almost all the crack under applied stress of 15kgf/mm².

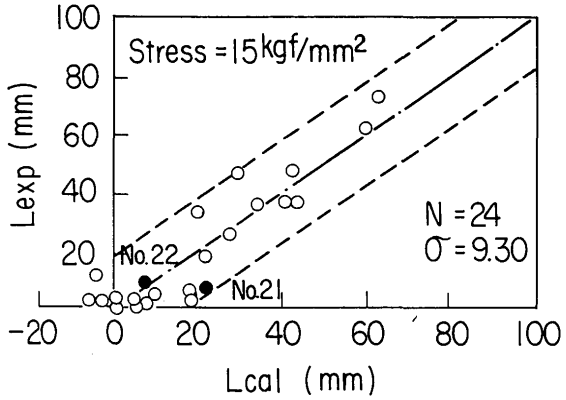

(a) base metal

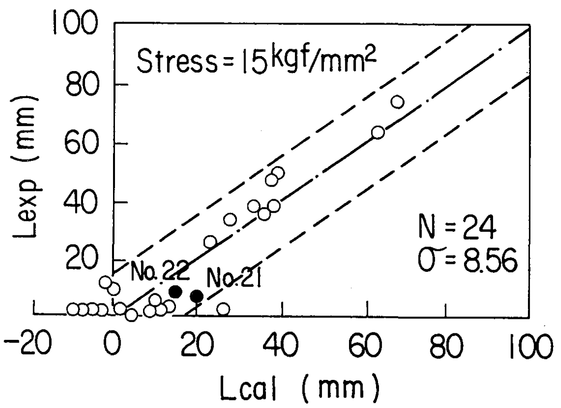

(b) weld metal

Fig. 8 Relation between calculated value (L_{cal}) of total crack length by the equation in Table 8 and measured value (L_{exp})

In the viewpoint of practical fabrication, the tensile stress acting to the weld section is different depending on the type of construction. Furthermore, the reduction of impurity elements to extremely low levels causes high manufacturing costs of the materials. Therefore it is necessary to select chemical composition suitable for the restraint condition of the practical construction. Thus the same materials as specimens No. 21 and 22 which have relatively enough properties against the ductility-dip crack was manufactured on practical production line, and were used for GT membrane type model tanks to confirm the practical applicability. The thickness of these materials is 0.5mm to 1.5mm, and pulsed TIG-arc welding and resistance seam welding were used.

Figure 9 shows the appearance of a part of the model tank. For inspection after the welding, color check and leakage check with Freon gas were utilized. **Table 9** shows the results of the inspection. The both materials showed good weldability, and no ductility-dip crack was observed. In Fig. 8 already shown the results of these materials are shown by solid circles. Therefore the material giving L_{exp} less than 10mm or L_{cal} less than 20mm has good resistance to the ductility-dip crack in actual fabrication, and furthermore can be made on manufactural production line.

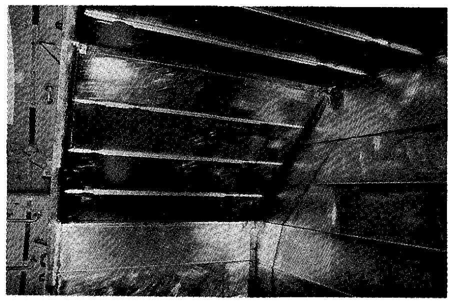

Fig. 9 LNG model tank (constructed by Hitachi Zosen Corp.)

Table 9 Results of inspections for model tanks

Specimen	Crack	Anti-leakage
No. 21	None	Good
No. 22	None	Good

3.4 Discussions

The regression analysis showed that S, O, N and Al serve as the crack-accelerating elements, and that also P accelerates a little, and that Si and Mn serve as the crack-inhibiting elements. The mechanism to cause this ductility-dip crack is considered to be that the harmful elements precipitate as some compounds or segregate on grain boundaries and thus weakens the strength of grain boundaries. Concerning this problem, it is reported that MnS and AlN precipitate on grain boundaries in simulated hot cracking test of Invar containing higher S and Al than commercial material[3, 4]. Any precipitates, however, has not been identified in commercial material, and thus the identification of precipitates or segregation on grain boundaries will be a future subject.

In order to prevent the crack, adequate selection of chemical composition is necessary. Concerning this problem, the equation in Table 8 is available to estimate the total crack length under the condition of applied stress of 15kgf/mm^2. Namely, the crack will never occur in the material which satisfy that $L_{cal} = 0$. However, technological and economical problems will arise, because such material contains extremely low impurity elements. In the case of GT type membrane tank for which the use of Invar has been planned, the material which satisfies the requirement of L_{exp} less than 10mm or L_{cal} less than 20mm should be selected, according to the results in model tanks. Also in the view of the strong effect of oxygen content in weld metal, special attention will have to be paid to the welding conditions. Since the air contamination into the shielding gas due to insufficient shielding gas causes an increase in the oxygen content in weld metal, welding should be done under sufficient gas shielding condition.

4. Conclusions

The results of Cross-bead type hot cracking test and regression analyses on the ductility-dip crack in the reheated weld metal, and the results obtained from the application to model tanks are summarized as follows:

1) Sulphur, oxygen, nitrogen and aluminum are the crack-accelerating elements, while phosphorus has a slight trend of crack-acceleration. On the other hand, silicon and manganese are the crack-inhibiting elements.

2) An estimating equation for the total crack length in Cross-bead test utilizing chemical composition was obtained under the condition of applied stress of $15 kgf/mm^2$. In this equation, it is better to use oxygen content in weld metal than that in base metal.

3) Materials having good properties against the crack was manufactured on practical production line, and applied to model tanks with good results.

Acknowledgement

The authors would like to thank Mr. S. Tomita who is the research student of Osaka Univ. for his cooperation.

References

1) H. Nakagawa, et al: Trans. JWRI, Vol. 9 (1980), No. 2, p. 197.

2) K. Nohara, et al: Tetsu to hagane, Vol. 66 (1980), No. 11, S1069 (in Japanese).

3) T. Kanamaru, et al: Tetsu to hagane, Vol. 70 (1984), No. 13, S1429 (in Japanese).

4) T. Okiyama, et al: Tetsu to hagane, Vol. 70 (1984), No. 13, S1430 (in Japanese).